

# Construction of paclitaxel-loaded poly (2-hydroxyethyl methacrylate)-g-poly (lactide)-1,2-dipalmitoyl-sn-glycero-3-phosphoethanolamine copolymer nanoparticle delivery system and evaluation of its anticancer activity

Xiaowei Ma\*  
Huan Wang\*  
Shubin Jin  
Yan Wu  
Xing-Jie Liang

Laboratory of Nanomedicine and Nanosafety, Division of Nanomedicine and Nanobiology, National Center for Nanoscience and Technology, People's Republic of China; and CAS Key Laboratory for Biomedical Effects of Nanomaterials and Nanosafety, Chinese Academy of Sciences, Beijing, People's Republic of China

\*These authors contributed equally to this work

**Background:** There is an urgent need to develop drug-loaded biocompatible nanoscale packages with improved therapeutic efficacy for effective clinical treatment. To address this need, a novel poly (2-hydroxyethyl methacrylate)-poly (lactide)-1,2-dipalmitoyl-sn-glycero-3-phosphoethanolamine [PHEMA-g-(PLA-DPPE)] copolymer was designed and synthesized to enable these nanoparticles to be pH responsive under pathological conditions.

**Methods:** The structural properties and thermal stability of the copolymer was measured and confirmed by Fourier transform infrared spectroscopy, nuclear magnetic resonance, and thermogravimetric analysis. In order to evaluate its feasibility as a drug carrier, paclitaxel-loaded PHEMA-g-(PLA-DPPE) nanoparticles were prepared using the emulsion-solvent evaporation method.

**Results:** The PHEMA-g-(PLA-DPPE) nanoparticles could be efficiently loaded with paclitaxel and controlled to release the drug gradually and effectively. In vitro release experiments demonstrated that drug release was faster at pH 5.0 than at pH 7.4. The anticancer activity of the PHEMA-g-(PLA-DPPE) nanoparticles was measured in breast cancer MCF-7 cells in vivo and in vitro. In comparison with the free drug, the paclitaxel-loaded PHEMA-g-(PLA-DPPE) nanoparticles could induce more significant tumor regression.

**Conclusion:** This study indicates that PHEMA-g-(PLA-DPPE) nanoparticles are promising carriers for hydrophobic drugs. This system can passively target cancer tissue and release drugs in a controllable manner, as determined by the pH value of the area in which the drug accumulates.

**Keywords:** poly (2-hydroxyethyl methacrylate), controlled release, biocompatibility, antitumor activity, 1,2-dipalmitoyl-sn-glycero-3-phosphoethanolamine, nanoparticles

Correspondence: Xing-Jie Liang  
CAS Key Laboratory for Biomedical Effects of Nanomaterials and Nanosafety, Chinese Academy of Sciences, Beijing 100190, People's Republic of China  
Email liangxj@nanoctr.cn

Yan Wu  
CAS Key Laboratory for Biomedical Effects of Nanomaterials and Nanosafety, Chinese academy of Sciences, Beijing 100190, People's Republic of China  
Email wuy@nanotr.cn

## Introduction

Scientists have been extensively researching ways to develop biocompatible and biodegradable drug carriers that possess certain clinically useful characteristics. Desirable characteristics include small particle size, high loading capacity, extended circulation time, ability to accumulate at pathological sites in the body, and the capacity to carry poorly soluble pharmaceuticals.<sup>1</sup> As nanotechnology develops, nanoparticles are becoming very attractive for drug delivery. Nanoparticles are able to reach tumors passively through the leaky vasculature surrounding the tumor tissue

via the enhanced permeation and retention effect.<sup>2</sup> Their prolonged circulation time gives the transported drug a better chance of reaching and/or interacting with its target tissue. Amphiphilic copolymers have attracted significant attention as carriers in drug delivery systems because they can form polymeric micelles by self-assembling in aqueous media. Polymeric micelles are composed of a hydrophilic shell and a hydrophobic core. They can thus enhance the solubility of poorly soluble drugs and increase their bioavailability. Further, they can circulate in the body or blood for a long time and accumulate to a greater extent in the target region. This allows for effective sustained release of the drug inside tumor tissue following accumulation of micelles in tumor tissue.<sup>3</sup>

Poly (2-hydroxyethyl methacrylate) (PHEMA) and its block copolymers have been widely used in the pharmaceutical industry because of their biocompatibility and environmental friendly characteristics. PHEMA can easily form hydrogels,<sup>4</sup> which are materials with a large number of biomedical applications due to their hydrophilic properties. Such applications include contact lenses, artificial implants, drug delivery systems, and nerve repair.<sup>5-9</sup> However, the mechanical properties of PHEMA hydrogels do not fit the requirements for many structural applications. Therefore, amphiphilic polymers consisting of PHEMA and biodegradable polyesters, ie, poly(L-lactide) (PLLA),<sup>10,11</sup> poly(D,L-lactide),<sup>12-14</sup> poly(glycolic acid), poly( $\epsilon$ -caprolactone),<sup>15,16</sup> and polystyrene, have been synthesized.<sup>17</sup> These copolymers can be obtained through ring-opening polymerization, atom transfer radical polymerization,<sup>11,18,19</sup> A<sub>2</sub>B<sub>2</sub> PCL/acrylate miktoarm polymers,<sup>20</sup> or use of a protective group, eg, a trimethylsilyl moiety.<sup>21</sup> The mechanical strength of the materials obtained is expected to be improved through synthesis of amphiphilic materials and combination of PHEMA hydrogels with hydrophobic components.

Poly(lactic acid) (PLA) is a biodegradable aliphatic polyester and it is one of the biocompatible polymers approved by the US Food and Drug Administration.<sup>22,23</sup> It has high mechanical strength, and excellent shaping and molding properties. Thus, it is widely used in medical fields for, eg, sustained drug delivery systems, implants for orthopedic devices, and absorbable fibers.<sup>24,25</sup> However, the low hydrophilicity and high crystallinity of PLA results in poor soft tissue compatibility.<sup>26</sup> Dipalmitoylphosphatidylethanolamine (DPPE) is the main constituent of the inner membranes of cells. Some laboratories have reported that polyethylene glycol-phosphatidylethanolamine (PEG-PE)

polymers can form stable micelles in aqueous media.<sup>27-29</sup> Their characteristic size, stability, and longevity in the systemic circulation make micelles containing a PE segment promising carriers for drug delivery to tumor tissue via the enhanced permeation and retention effect.<sup>27-29</sup> Amphiphilic triblock copolymers could interact with the phospholipid monolayer membranes of dipalmitoylphosphatidylcholine (DPPC) and dimyristoylphosphatidylcholine (DMPC).<sup>30</sup> Introduction of the PE segment could increase the internalization of drug-loaded micelles into lysosomes by tumor cells and therefore enhance cytotoxicity.<sup>29</sup> However, PEG-PE copolymers are expensive. Another drawback of PEG-based copolymers is the absence of reactive groups on their molecular chains, which limits further modification or ligand coupling.

Solid tumors account for more than 85% of cancer mortality. The commercial formulation of paclitaxel (Taxol<sup>®</sup>) is dissolved in a 50:50 v/v mixture of Cremophor EL and dehydrated alcohol, and is very effective in the treatment of a broad range of solid tumors. However, its use is greatly limited by its poor solubility. Further, the Cremophor EL-based formulation of paclitaxel often has serious side effects in patients, including allergic reactions, neurotoxicity, and nephrotoxicity.<sup>31</sup> Due to these serious problems, a delivery system that improves the solubility of paclitaxel and decreases its toxicity needs to be developed. There have been many attempts to formulate paclitaxel into a delivery system that does not require Cremophor for solubilization. A number of alternative submicronic colloidal systems have been developed, including liposomes, microspheres, and polymeric micelles.<sup>32</sup> However, the available optimized paclitaxel-based delivery systems (eg, albumin-bound paclitaxel nanoparticle formulations) for clinical application are very limited.

In the present work, we successfully synthesized a PHEMA-g-(PLA-DPPE) copolymer using a three-step process. We did so in order to combine the advantages of PHEMA and DPPE to form an antitumor drug (paclitaxel) carrier. Further, the chemical structure and physicochemical properties of the copolymers were investigated. It was found that paclitaxel could be loaded and incorporated into polymeric PHEMA-g-(PLA-DPPE) nanoparticles by an emulsion-solvent evaporation technique. We also investigated the physicochemical properties of these paclitaxel-loaded polymeric nanoparticles, including their size, loading content, encapsulation efficiency, and paclitaxel release profile. The potential of these nanoparticles as efficient paclitaxel carriers was also evaluated. The in vitro cytotoxic activity and in vivo antitumor efficiency of

the paclitaxel-loaded PHEMA-g-(PLA-DPPE) nanoparticles were evaluated in human breast cancer-bearing nude mice models. The results were compared with the antitumor efficiency of free paclitaxel in the same conditions.

## Materials and methods

### Experimental materials

PHEMA (molecular weight 20 kDa), 1, 2-dipalmitoyl-sn-glycero-3-phosphoethanolamine, and triethylamine were purchased from Sigma Chemical Co (St Louis, MO). DL-Lactide (DLA), 4-nitrophenyl chloroformate (pNP), and 4-dimethylaminopyridine were obtained from Alfar Aesar (Ward Hill, MA). Paclitaxel was purchased from Beijing HuaFeng United Technology Co, Ltd (Beijing, China). Cremophor EL was purchased from Aladdin Chemistry Co, Ltd (Collierville, TN). Dulbecco's Modified Eagle's Medium and fetal bovine serum were obtained from Hyclone (Logan, UT). All solutions were prepared with Milli-Q water ( $18 \text{ M}\Omega \text{ cm}^{-1}$ ) from a Millipore system (Billerica, MA). All other chemical reagents were analytical grade and used as received.

### Synthesis of PHEMA-g-(PLA-DPPE) copolymer

Synthesis of the PHEMA-g-(PLA-DPPE) copolymer was a three-step process that can be described as follows. The PHEMA-PLA was synthesized by a previous reported one-step ring-opening polymerization method,<sup>33</sup> with some changes. Briefly, 10 g of DLA was added to 500 mg of PHEMA-dimethyl sulfoxide (DMSO) solution by stirring, and then 0.01 mol triethylamine was added dropwise. The solution was reacted at  $86^{\circ}\text{C}$  by magnetic stirring under a nitrogen atmosphere. After 12 hours, the reacted solution was added to iced water and the precipitate was collected and thoroughly washed with distilled water three times. Finally, the raw product obtained was extracted with toluene. The pure PHEMA-PLA copolymer was dried at  $40^{\circ}\text{C}$  for 48 hours under vacuum.

Activation of PHEMA-PLA to PHEMA-PLA-pNP was performed as described by Wang et al,<sup>34</sup> with some modifications. Briefly, 1.1 g of PHEMA-PLA was dissolved in 6 mL of chloroform by stirring, and then 0.5 g of pNP, 40 mg of 4-dimethylaminopyridine (dissolved in 6 mL of chloroform), and 1 mL of pyridine were added to the solution. The reaction took place at  $0^{\circ}\text{C}$  for 6 hours and at room temperature for 12 hours by magnetic stirring. The resulting product was added to diethyl ether-petroleum ether (2:1, v/v), and the precipitate was collected and washed with the

mixed ether three times. The pure product was dried under vacuum for 48 hours.

The PHEMA-g-(PLA-DPPE) copolymer was synthesized as follows. A mixture of PHEMA-PLA-pNP and DPPE (containing a measured amount of triethylamine) with a feed weight ratio of 20:1–50:1 (PHEMA-PLA-pNP/DPPE) was suspended in 20 mL of chloroform with magnetic stirring at  $25^{\circ}\text{C}$  in the absence of light. After being stirred continuously for 12 hours, the resulting product was added to diethyl ether-petroleum ether (1:1, v/v). The precipitate was collected and washed with the mixed ether three times. The PHEMA-g-(PLA-DPPE) obtained was dried under vacuum for 48 hours.

### Characterization of PHEMA-g-(PLA-DPPE) copolymer

The chemical compositions of PHEMA and PHEMA copolymers were recorded using Fourier transform infrared spectroscopy (Perkin-Elmer, Fremont, CA). PHEMA and its copolymers were mixed with KBr and then pressed into a disk for measurement. Nuclear magnetic resonance (NMR) was also used to confirm the structure of the copolymers.  $^1\text{H}$  NMR,  $^{13}\text{C}$  NMR, and  $^{31}\text{P}$  NMR spectra were recorded on a Bruker Avance 400 NMR spectrophotometer (Billerica, MA), with  $\text{DMSO}-d_6$  as the solvent. The thermal stability of the samples were measured by thermogravimetric analysis using Perkin-Elmer Instruments with a heating rate of  $20^{\circ}\text{C}$  per minute under a nitrogen atmosphere from  $25^{\circ}\text{C}$  to  $900^{\circ}\text{C}$ . Molecular weight and polydispersity were detected using gel permeation chromatography (Waters 2410, Milford, MA).

### Construction and characterization of paclitaxel-loaded copolymer nanoparticles

An emulsion-solvent evaporation method was used to prepare the paclitaxel-loaded PHEMA-g-(PLA-DPPE) nanoparticles as previously described.<sup>35</sup> Briefly, 10 mg of PHEMA-g-(PLA-DPPE) (20:1) copolymer was dissolved in 1.5 mL of methylene chloride. Paclitaxel (1 mg/mL in methylene chloride) was added at mass ratios of copolymer:paclitaxel of 100/1, 70/1, and 50/1. The mixture was poured into 10 mL of 0.5%–2.0% (w/v) polyvinyl alcohol solution, stirred for 10 minutes at room temperature, and then sonicated (50 w) for 5 minutes. The solvent was rapidly eliminated by evaporation. Finally, the nanoparticles were collected by centrifugation at 12,000 rpm for 5 minutes at room temperature and washed three times with water.

## Loading content and encapsulation efficiency of paclitaxel-loaded nanoparticles

The drug-loading content and encapsulation efficiency of the nanoparticles were determined by high performance liquid chromatography (HPLC, water, 626/2478). Briefly, 6 mg of lyophilized nanoparticles were dissolved in 1 mL of acetonitrile under vigorous vortexing, and the clear solution was obtained for HPLC analysis. The mobile phase of HPLC was composed of acetonitrile:water 80/20 (v/v). The flow rate was 1.0 mL/minute at 25°C, and the wavelength was set at 227 nm. The paclitaxel-loading content and encapsulation efficiency of the nanoparticles were calculated as follows:

$$\text{Paclitaxel-loading content} = \frac{\text{Amount of paclitaxel in nanoparticles}}{\text{Amount of nanoparticles after lyophilization}} \times 100\% \quad (1)$$

$$\text{Encapsulation efficiency} = \frac{\text{Amount of paclitaxel in nanoparticles}}{\text{Initial amount of paclitaxel in the system}} \times 100\% \quad (2)$$

## PHEMA-g-(PLA-DPPE) nanoparticle size and distribution

The particle size and size distribution was measured using a Zetasizer NanoZS analyzer (Malvern Instruments Ltd, Worcestershire, UK) using the dynamic light scattering technique. The nanoparticles were appropriately diluted with distilled water. Determinations were performed at 633 nm with a constant angle of 90 degrees at 25°C.

## Morphology of PHEMA-g-(PLA-DPPE) nanoparticles

The morphology of the nanoparticles was observed by transmission electron microscopy (TEM, Tecnai G<sup>2</sup> 20, Eindhoven, The Netherlands). For the TEM experiments, a drop of the sample solution was allowed to settle on a copper grid and the sample was air-dried. The nanoparticles were examined using TEM by negative staining with uranyl acetate.

## In vitro drug release

Drug release experiments were carried out in vitro as follows. A 12 mg sample of lyophilized paclitaxel-loaded PHEMA-g-(PLA-DPPE) nanoparticles was dispersed in 5 mL of phosphate-buffered saline and then introduced into dialysis bags (molecular weight 3500 g/mol). The dialysis bags were placed into 35 mL of phosphate-buffered saline (pH 7.4 or pH 5.0),

and the media was stirred at 100 rpm and 37°C in a water bath. A 1 mL sample was then taken out for analysis of paclitaxel concentration at specific time intervals. Thereafter, 1 mL of the media was replaced with fresh distilled water. The concentration of paclitaxel released was determined using HPLC (Agilent 1200 Infinity LC, Santa Clara, CA).

## Cytotoxicity assay

The inhibitory effects of the paclitaxel-loaded nanoparticles on human breast cancer cells were measured. MCF-7 cells were seeded into 96-well culture plates at 5000 cells/well and cultured at 37°C in a humidified atmosphere with 5% CO<sub>2</sub> for overnight to allow for cell attachment. The cells were then exposed to a series of concentrations of free paclitaxel (DMSO < 1%) and paclitaxel-loaded nanoparticles. The final concentration of paclitaxel was in the range of 0.001–50 µg/mL. The cells were further incubated for 48 hours and cytotoxicity was assessed using CCK-8 kits (Dojindo Molecular Technologies, Tokyo, Japan).

## Inhibition efficacy in breast cancer xenografts by intraperitoneal delivery

Female nu/nu nude mice (initially weighing 18–20 g and purchased from Beijing Vital River Company, Beijing, China) were used to investigate antitumor efficacy in vivo. The animals were housed under standard conditions with free access to food and water. All animal experiments were performed in accordance with the principles of care and use of laboratory animals. Briefly, approximately  $2 \times 10^6$  MCF-7 cells were resuspended in 100 µL of physiological saline, and injected subcutaneously into the right flanks of the nude mice. When tumors reached 50–70 mm<sup>3</sup> in volume, the mice were randomly divided into three treatment groups (four mice per group). At days 7, 14, 21, 28, and 35 following inoculation, the physiological saline, Taxol 10 mg/kg, and paclitaxel-loaded nanoparticles (administered at a paclitaxel-equivalent dose of 10 mg/kg) were administered intraperitoneally to the mice in the three treatment groups. Tumor progression in the mice was then monitored every four days. Tumor volumes were calculated as  $\text{length} \times \text{width}^2/2$  (mm<sup>3</sup>). The mice were sacrificed at the end of the experiment, and their tumors were immediately removed and weighed.

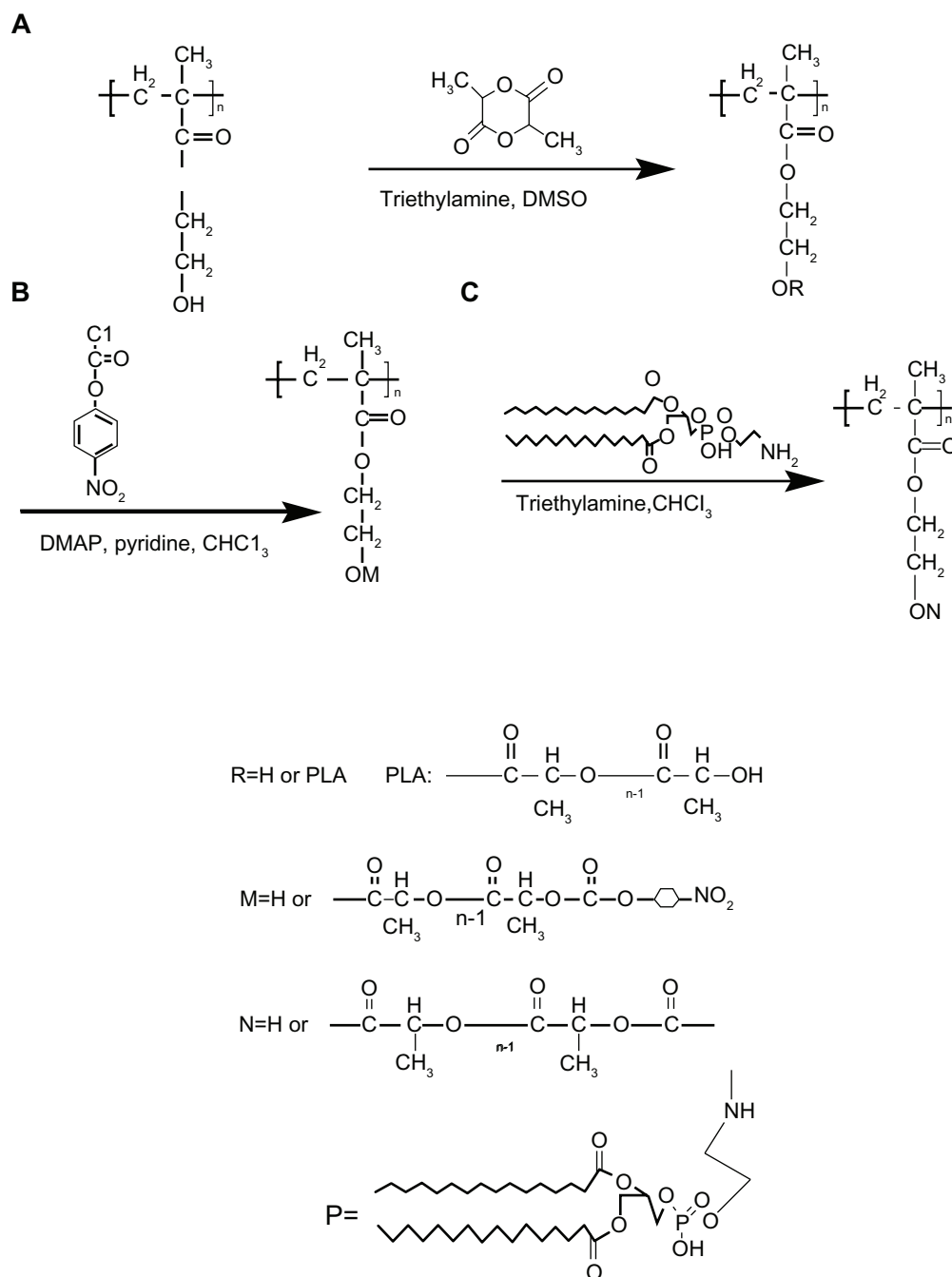
## Results

### Synthesis and characterization of copolymer

PHEMA and PLA are two well established polymer materials and have been widely used in the medical and health care fields.

DMSO is a good solvent for PHEMA at room temperature. In this study, we first synthesized PHEMA-PLA, a poly (lactide)-poly (2-hydroxyethyl methacrylate) grafted copolymer, via a one-step ring-open polymerization method (Schema 1A). The molecular weight and polydispersity index of the PHEMA-PLA (PHEMA to DLLA 1:20) were 38 kDa and 1.28, respectively (determined by gel permeation chromatography). The method used was different from other

previously reported methods.<sup>11,12,14</sup> In the present work, pNP was selected for activation of the PHEMA-PLA copolymer (Schema 1B) according to a previously reported method, with some changes.<sup>34</sup> The content of 4-nitrophenyl carbonate moieties could be determined during the reaction course. The degree of 4-nitrophenyl carbonate substitution could be controlled by adjusting the amount of chloroformate added. Finally, PHEMA-g-(PLA-DPPE) was synthesized in the



**Schema 1** Synthetic route for (A) PHEMA-PLA, (B) PHEMA-PLA-pNP, and (C) PHEMA-g-(PLA-DPPE).

**Abbreviations:** PHEMA, poly (2-hydroxyethyl methacrylate); PLA, poly (lactide)-I; DPPE, 2-dipalmitoyl-sn-glycero-3-phosphoethanolamine; pNP, 4-nitrophenyl chloroformate.

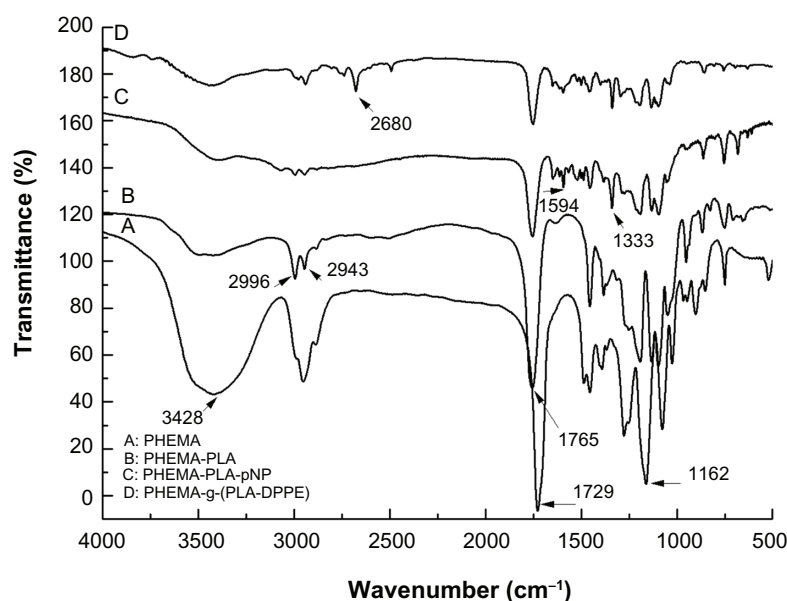


presence of triethylamine. The polymerization route is shown in Schema 1C. The molecular weight and polydispersity of the PHEMA-g-(PLA-DPPE) (PHEMA-PLA-pNP to DPPE 20:1) were 43 kDa and 1.34, respectively (determined by gel permeation chromatography). The final products of PHEMA-g-(PLA-DPPE) had good solubility in  $\text{CH}_2\text{Cl}_2$ ,  $\text{CHCl}_3$ , acetone, and DMSO. The chemical structure and physicochemical properties of PHEMA and their copolymers were confirmed by Fourier transform infrared spectroscopy,  $^1\text{H}$  NMR,  $^{13}\text{C}$  NMR,  $^{31}\text{P}$  NMR, and thermogravimetric analysis (some detailed descriptions and figures are shown in the supplementary section).

Figure 1 shows the Fourier transform infrared spectra for the PHEMA, PHEMA-PLA, PHEMA-PLA-pNP, and PHEMA-g-(PLA-DPPE) copolymers, respectively. In Figure 1A, the absorption peak appearing at approximately  $1729\text{ cm}^{-1}$  corresponds to the carbonyl group of the branched PHEMA; the bands at  $3428\text{ cm}^{-1}$  and  $1162\text{ cm}^{-1}$  were attributed to the O–H and the C–O stretching vibration, respectively. Compared with the Fourier transform infrared spectra of PHEMA, the absorption peak at  $1729\text{ cm}^{-1}$  transferred to  $1765\text{ cm}^{-1}$  in the PHEMA-PLA (Figure 1B). These results reflect the different location of the carbonyl group in the polymers. The intensity of the peak at  $3428\text{ cm}^{-1}$  was weaker and wider after grafting of PLA. These results indicate that some changes occurred after grafting PLA onto the –OH of PHEMA. In Figure 1B, absorption peaks at about  $2996\text{ cm}^{-1}$  and about  $2943\text{ cm}^{-1}$  were attributed to  $-\text{CH}_2$  absorption. In

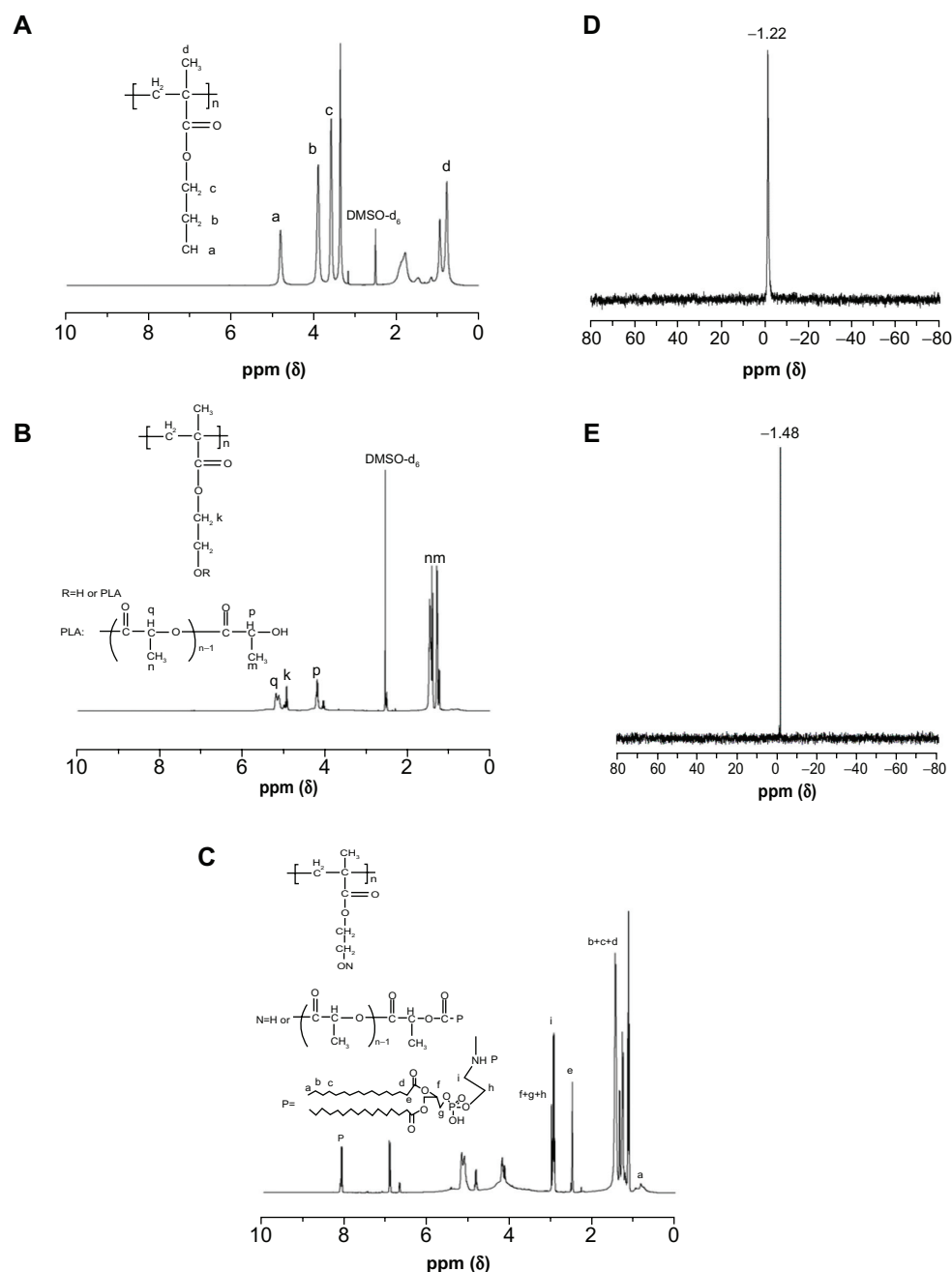
Figure 1C, the peak appearing at about  $1754\text{ cm}^{-1}$  was attributed to 4-nitrophenyl carbonate, and this peak was overlapping with the carbonyl group absorption peak at  $1765\text{ cm}^{-1}$ . The peaks at approximately  $1594\text{ cm}^{-1}$  and about  $1333\text{ cm}^{-1}$  corresponded to  $-\text{NO}_2$  stretching vibration. In the PHEMA-g-(PLA-DPPE) copolymer, the peak at about  $2680\text{ cm}^{-1}$  was attributed to PO–H stretching vibration (Figure 1D). All these results demonstrate that the intended copolymer had been obtained.

Figure 2 shows the  $^1\text{H}$  NMR spectra of PHEMA, PHEMA-PLA, and the PHEMA-g-(PLA-DPPE) copolymer, respectively. Compared with PHEMA (Figure 2A), the  $^1\text{H}$  NMR spectra of the PHEMA-PLA copolymer (Figure 2B) indicate that the signals at about 1.3 and 1.5 ppm are attributable to the methyl protons of the PLA moiety located in the terminal groups and repeat units. The signals at about 4.2 and 5.1 ppm were attributed to the methine (CH) protons of the PLA moiety located in the terminal groups and repeat units. All these results confirm that the PHEMA derivatives contained a PLA side chain.<sup>14,15</sup> In the  $^1\text{H}$  NMR spectra of the PHEMA-g-(PLA-DPPE) copolymer (Figure 2C), the signal at about 0.9 ppm was attributed to the terminal methyl proton of the DPPE moiety. Peaks at 1.2–1.6 ppm were attributed to methyl protons of the DPPE moiety. The signal at about 8.2 ppm was assigned to the proton of –NH in the DPPE moiety. All other absorption peaks were attributed to protons of the DPPE moiety. Further, typical  $^{31}\text{P}$  NMR spectra of DPPE and the PHEMA-g-(PLA-DPPE) copolymer were recorded and are shown in Figure 2D and E.



**Figure 1** Fourier transform infrared spectra of (A) PHEMA, (B) PHEMA-PLA, (C) PHEMA-PLA-pNP, and (D) PHEMA-g-(PLA-DPPE).

**Abbreviations:** PHEMA, poly (2-hydroxyethyl methacrylate); PLA, poly (lactide)-I; DPPE, 2-dipalmitoyl-sn-glycero-3-phosphoethanolamine; pNP, 4-nitrophenyl chloroformate.



**Figure 2** <sup>1</sup>H NMR spectra of (A) PHEMA, (B) PHEMA-PLA, and (C) PHEMA-PLA-DPPE, and (D) <sup>31</sup>P NMR spectrum of (E) DPPE and PHEMA-g-(PLA-DPPE) copolymer. **Abbreviations:** PHEMA, poly (2-hydroxyethyl methacrylate); PLA, poly (lactide)-I; NMR, nuclear magnetic resonance; DPPE, 2-dipalmitoyl-sn-glycero-3-phosphoethanolamine; pNP, 4-nitrophenyl chloroformate.

Compared with DPPE (Figure 2D), the <sup>31</sup>P NMR spectra of the PHEMA-g-(PLA-DPPE) copolymer (Figure 2E) show a peak at about 1.48 ppm that is generally expected for <sup>31</sup>P functionalities.<sup>36,37</sup> The <sup>31</sup>P NMR spectra confirm that phosphate groups were chemically bonded to the material.

## Characterization of nanoparticles

In this study, PHEMA, PLA, and DPPE were used to form size-controllable nanoparticles with potential for

pharmaceutical application. Given that PE is the main constituent of the inner membrane of the cell, introducing DPPE into the copolymer may help to enhance the biocompatibility of the nanoparticles. In addition, according to previous research, the PE-containing DPPE segment fused rapidly when the medium pH was lowered from 7.0 to 5.0, and drug release increased during fusion of the materials. Previously published reports have also shown that PE is a pH-sensitive lipid component and has been used to trigger and enhance

drug release by liposomes. The hydrophobic segment (or anthracene ring) of an antitumor drug can interact with DPPE phospholipids upon encapsulation in nanoparticles, such that the drug has a higher encapsulation efficiency and loading content in the nanoparticles when the materials contain DPPE.<sup>29,38,39</sup>

PHEMA was chosen for the hydrophilic phase because of its biocompatibility, hydrophilicity, softness, high water content, and permeability. Because the primary purpose of this study was to deliver hydrophobic paclitaxel, as shown schematically in Figure 3A, an emulsion-solvent evaporation method was chosen to prepare the paclitaxel-loaded nanoparticles. In a previous study, we showed that increasing the amount of PLA led to a highly viscous copolymer solution, which resulted in an increased particle size (data not shown). As a result, we chose a fixed ratio (1:20) of PHEMA-DLLA for conjugation of DPPE onto PHEMA-PLA and 20:1 of PHEMA-PLA-pNP to DPPE for balancing the loading of drug and controlling the size of the resulting nanoparticles. The drug-loaded nanoparticles were lyophilized for longer storage and could be subsequently redissolved in water or phosphate-buffered saline for further use.

TEM was used to examine the morphology of empty PHEMA-g-(PLA-DPPE) nanoparticles and paclitaxel-loaded PHEMA-g-(PLA-DPPE) nanoparticles. The TEM images demonstrated that the nanoparticles became dispersed as individual particles with a typical spherical shape. They were homogeneously distributed around a size of 120–225 nm, as shown in Figure 3B (a and c). Dynamic light scattering was used to determine the average hydrodynamic diameters of the resulting nanoparticles. The diameters were approximately 170 nm, as shown in Figure 3B (b) and 240 nm as shown in Figure 3B (d) for empty PHEMA-g-(PLA-DPPE) nanoparticles and paclitaxel-loaded PHEMA-g-(PLA-DPPE) nanoparticles in water, respectively. The diameter observed by TEM was smaller than that detected by the Zetasizer NanoZS analyzer. This is because the diameter obtained by dynamic light scattering reflects the hydrodynamic diameter of nanoparticles swelling in aqueous solution. However, the diameter observed by TEM is the diameter of the dried nanoparticle.

## Formulation parameters and size, loading content, and encapsulation efficiency

Size distribution (polydispersity index), paclitaxel-loading content, and encapsulation efficiency play an important role in in vitro studies and in vivo applications of drug-loaded

nanoparticles. The effects of formulation parameters on size, drug-loading content, and encapsulation efficiency in this study are shown in Table 1. Size and size distribution of the nanoparticles was determined by dynamic light scattering. The results show the effect of the feed mass ratio of copolymer to paclitaxel on the size of the paclitaxel-loaded nanoparticles, which gradually increased as the paclitaxel content increased. After loading with paclitaxel, the nanoparticle size increased. When the initial paclitaxel feed amounts were varied, the size and loading content changed. Specifically, the higher the feed amount of paclitaxel, the larger the size and higher the paclitaxel loading content that was obtained (Table 1). This result is expected, because incorporation of paclitaxel into the hydrophobic cores increased with nanoparticle volume. The size difference before and after drug loading suggests that hydrophobic drug-loading increased the size of the nanoparticles. The same results were also observed in previous studies using other types of drugs.<sup>40</sup>

Polyvinyl alcohol was used in the current study as an emulsifier. As can be seen from Table 1, the mean diameter and polydispersity index of the nanoparticles, encapsulation efficiency, and loading content were investigated at different copolymer-drug ratios and polyvinyl alcohol concentrations. The viscosity of the suspension was significantly increased at high polyvinyl alcohol concentrations, which decreased the loading content and encapsulation efficiency. In our experiment, at every copolymer-drug ratio, increased nanoparticle size, decreased encapsulation efficiency, and decreased loading content was observed with increasing polyvinyl alcohol concentrations. In addition, too much polyvinyl alcohol should not be taken into the nanoparticles because it could not be totally biodegraded in vivo and was difficult to remove. Therefore, 0.5% polyvinyl alcohol was used for preparing the nanoparticles. At a copolymer-drug ratio of 100:1, the nanoparticles had the smallest size and polydispersity index, indicating their uniform distribution in solution. Therefore, a copolymer-drug ratio of 100:1 and 0.5% was chosen for further biological study, with relatively high encapsulation efficiency and a loading content of 53.9% and 0.60%, respectively.

## Controlled in vitro drug release from nanoparticles

It has been demonstrated that controlled and continuous drug release is essential for successful use of pharmaceuticals.<sup>41</sup> Figure 4 shows the in vitro release profiles for paclitaxel from nanoparticles. In all the curves, a burst effect was



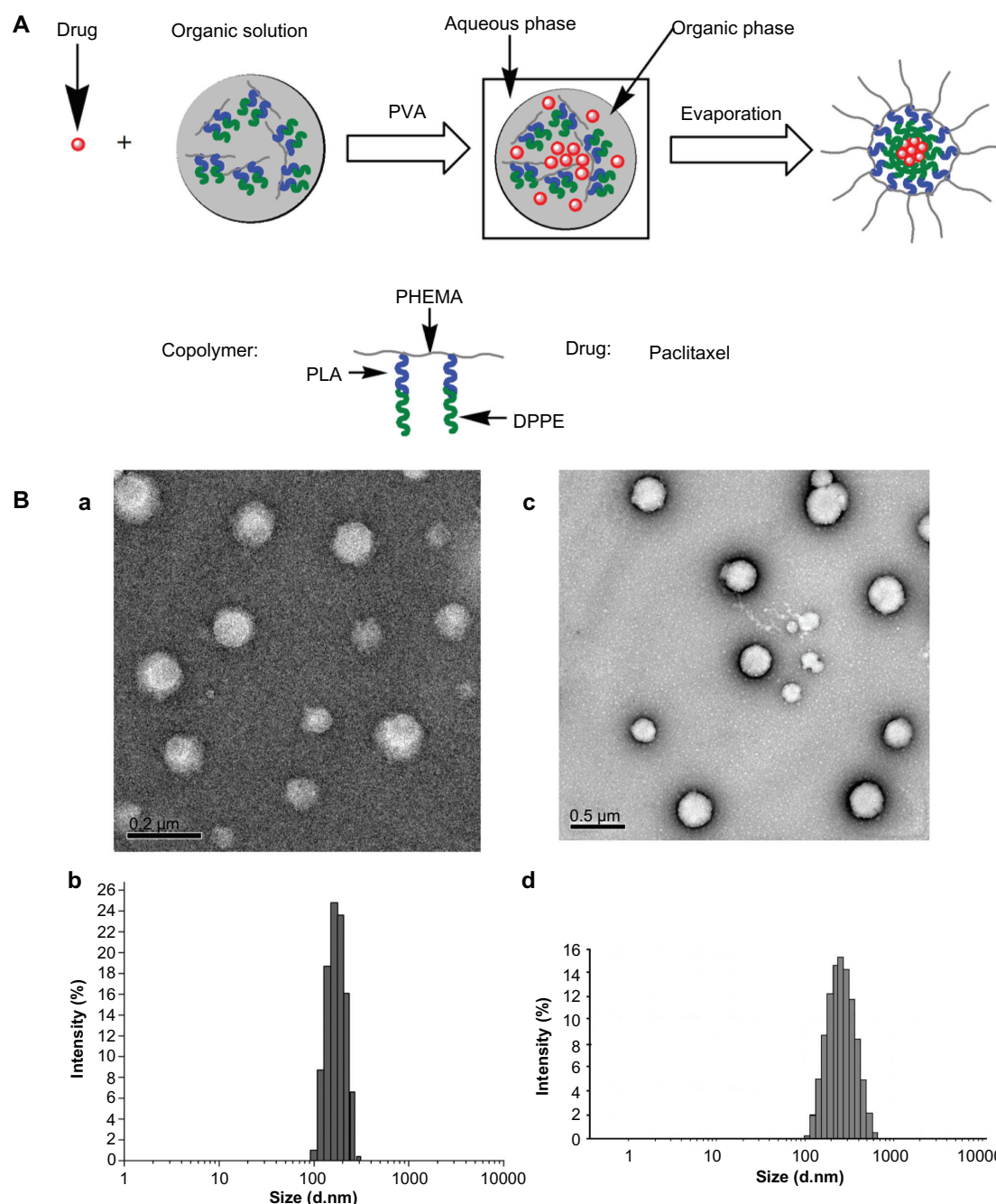


**Figure 3** Schematic illustration of paclitaxel encapsulation into nanoparticles with the PHEMA-g-(PLA-DPPE) copolymer by emulsion/solvent evaporation (**A**) and transmission electron microscopy and dynamic light scattering characterization of empty and paclitaxel-loaded nanoparticles made by the emulsion/solvent evaporation method (**B**). Transmission electron microscopic image (**a**) and dynamic light scattering histogram, (**b**) of empty nanoparticles; transmission electron microscopic image (**c**) and dynamic light scattering histogram (**d**) of paclitaxel-loaded nanoparticles.

**Abbreviations:** PHEMA, poly (2-hydroxyethyl methacrylate); PLA, poly (lactide)-I; DPPE, 2-dipalmitoyl-sn-glycero-3-phosphoethanolamine.

observed within the first 24 hours. This was followed by a slow continuous release over the next 12 days at both pH 7.4 and pH 5.0. This sustained release could result from diffusion of paclitaxel into the polymer wall, diffusion of the drug through the polymer wall, and erosion of the polymer. Drug release from copolymer nanoparticles is a rather complicated process. It can be affected by many factors, including polymer

degradation, molecular weight, crystallinity, and the binding affinity between polymer and drug. In this study, the drug release rate might have been determined mainly by diffusion of the drug through the polymer matrix. The initial burst release of paclitaxel from the nanoparticles may be attributable to the diffusion of paclitaxel located in close proximity to the surface of the PHEMA-g-(PLA-DPPE) nanoparticles.

**Table I** Effects of formulation parameters on size, size distribution, loading content of paclitaxel, and encapsulation efficiency of paclitaxel-loaded PHEMA-g-(PLA-DPPE) nanoparticles

| Copolymer:drug ratio | 100:1         | 70:1          | 50:1          |
|----------------------|---------------|---------------|---------------|
| 0.5%PVA              |               |               |               |
| Mean diameter (nm)   | 239.8 ± 2.1   | 249.2 ± 1.6   | 257.3 ± 3.1   |
| PDI                  | 0.114 ± 0.006 | 0.133 ± 0.008 | 0.189 ± 0.011 |
| EE (%)               | 53.90 ± 1.4   | 57.30 ± 1.2   | 67.00 ± 2.3   |
| LC (%)               | 0.60 ± 0.15   | 0.98 ± 0.17   | 1.65 ± 0.13   |
| 1%PVA                |               |               |               |
| Mean diameter (nm)   | 250.0 ± 2.3   | 259.5 ± 3.1   | 269.0 ± 4.0   |
| PDI                  | 0.106 ± 0.004 | 0.151 ± 0.012 | 0.243 ± 0.010 |
| EE (%)               | 48.00 ± 1.2   | 51.00 ± 1.7   | 63.00 ± 2.5   |
| LC (%)               | 0.52 ± 0.13   | 0.85 ± 0.12   | 1.34 ± 0.16   |
| 2%PVA                |               |               |               |
| Mean diameter (nm)   | 269.2 ± 3.4   | 295.6 ± 2.5   | 301.2 ± 2.2   |
| PDI                  | 0.211 ± 0.013 | 0.224 ± 0.009 | 0.253 ± 0.120 |
| EE (%)               | 42.40 ± 2.1   | 50.60 ± 1.9   | 61.00 ± 2.4   |
| LC (%)               | 0.39 ± 0.11   | 0.67 ± 0.13   | 1.18 ± 0.12   |

**Abbreviations:** PHEMA, poly (2-hydroxyethyl methacrylate); PLA, poly (lactide)-I; DPPE, 2-dipalmitoyl-sn-glycero-3-phosphoethanolamine.

The PHEMA-g-(PLA-DPPE) copolymer under optimal delivery conditions would facilitate drug diffusion from the nanoparticle cores. At pH 5.0 and pH 7.4, release of paclitaxel from the nanoparticles over 12 days was 86.90% and 37.8%, respectively. These observations demonstrated that at pH 5.0, paclitaxel was released much faster from the nanoparticles than it was at pH 7.4. Our results are in agreement with previously published reports indicating that PE is a pH-sensitive lipid component.<sup>42</sup> Furthermore, the slowly controlled release of paclitaxel from the nanoparticles at pH 7.4 indicates that the paclitaxel-loaded nanoparticles are stable during circulation in the blood. Incorporation of paclitaxel in nanoparticles could reduce systemic toxicity due to slower release in neutral body fluid.

## Nanoparticle cytotoxicity in vitro and in vivo

To investigate the biological safety of PHEMA-g-(PLA-DPPE) nanoparticles further, a blood smear test was performed to determine if these nanoparticles can induce hemolysis in mice. Red blood cell morphology was observed after treating the mice with blank PHEMA-g-(PLA-DPPE) nanoparticles or incubating normal mice blood with different concentrations of PHEMA-g-(PLA-DPPE) copolymers. As can be seen from Figure 4B, no alteration in erythrocyte morphology was found in any of the treatment groups, indicating that the nanoparticles have favorable blood compatibility.

Our nanoparticle formulation was assessed for its activity in cell culture. To compare the cytotoxicity of encapsulated and free paclitaxel, effects on cellular proliferation were examined using MCF-7 cells (Figure 5A). After treatment with free paclitaxel and paclitaxel-loaded nanoparticles, the proliferation of MCF-7 cells was quantified. Importantly, cells retained high viability after 48 hours in the presence of the empty nanoparticles at different concentrations under the experimental conditions. These results demonstrated that this nanoparticle formulation was not inherently cytotoxic.

Both the free paclitaxel and paclitaxel-loaded nanoparticles significantly reduced tumor cell numbers in a concentration-dependent manner as compared with the controls. In fact, the cytotoxic activity of the paclitaxel-loaded nanoparticles and free paclitaxel showed equivalent trends in vitro, with IC<sub>50</sub> values of 0.061 µg/mL for the free drug and 0.050 µg/mL for the polymeric paclitaxel-loaded nanoparticles. These data, together with the in vitro drug release results, suggest enhanced antitumor efficacy by the nanoparticle delivery route in vivo.

Paclitaxel-loaded nanoparticles were next evaluated for their antitumor activity. The tumor volume growth curve (Figure 5B) shows that both free paclitaxel and the paclitaxel-loaded nanoparticles effectively inhibited MCF-7 tumor growth, while the tumor growth rate in mice receiving paclitaxel-loaded nanoparticle treatment was much lower than in mice receiving treatment with free paclitaxel. Figure 5C shows statistical analysis of tumor weights from the different treatment groups after sacrificing the mice at the end of the experiment. The results show that, compared with free paclitaxel (inhibition rate 45.42%), the inhibition rate in the group treated with paclitaxel-loaded nanoparticles was significantly increased to 63.65% ( $P < 0.05$ ). Representative images of excised tumors from mice receiving different treatment are shown in Figure 5D.

## Discussion

Circumventing the deficiencies of first-line anticancer agents has not only scientific importance but also clinical significance. Solubility of the compound is important for the chemotherapeutic agent to take effect. About half of the potentially valuable drug candidates identified by high throughput screening technology (including those with the highest activity) demonstrate poor solubility in water. For this reason, the drugs are not developed further, and do not enter a formulation development stage.<sup>2</sup> Paclitaxel is one of the most effective chemotherapeutic drugs in treating a variety of cancers. However, chemotherapy with paclitaxel has been

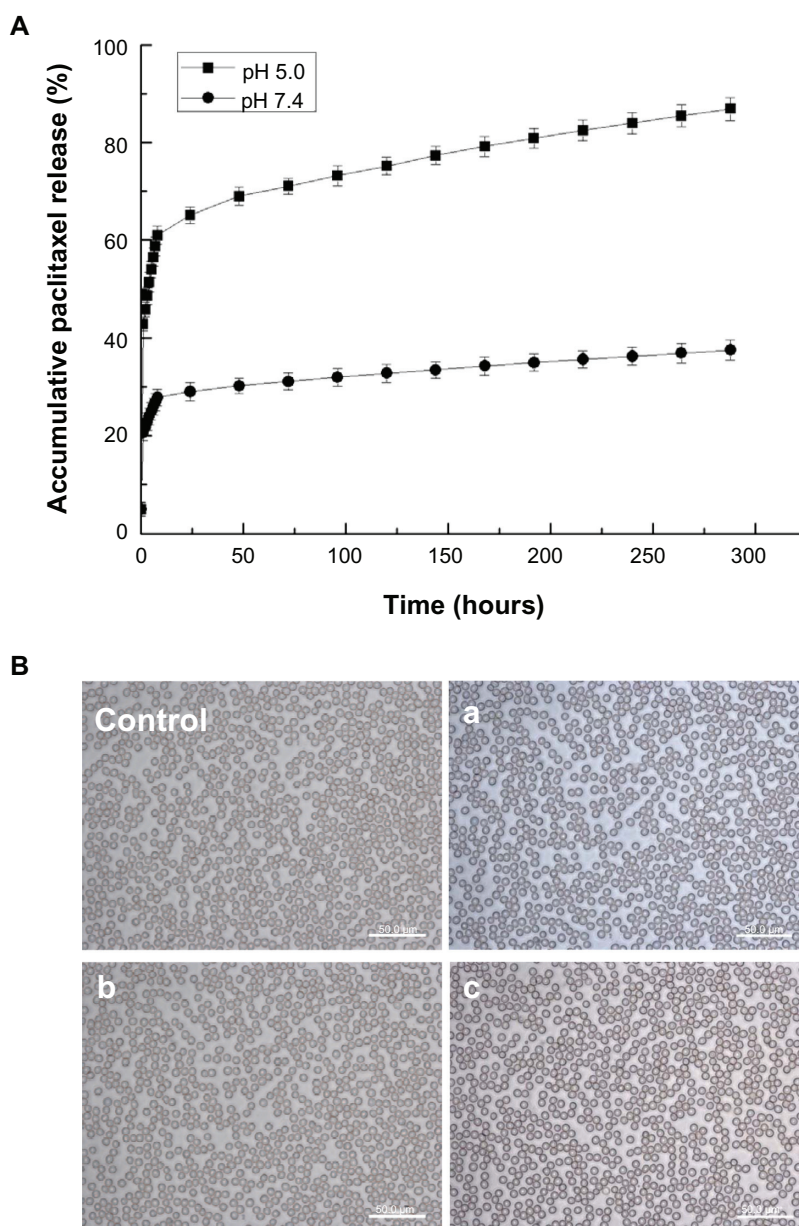


**Figure 4 (A)** Accumulative release profiles of paclitaxel and paclitaxel-loaded nanoparticles at different pH values (copolymer/drug 100:1, polyvinyl alcohol 0.5%). **(B)** Effects of PHEMA-g-(PLA-DPPE) nanoparticles on erythrocyte morphology. Control: erythrocyte morphology in normal mice blood (a); erythrocyte morphology in mice after receiving blank PHEMA-g-(PLA-DPPE) nanoparticle treatment via intraperitoneal injection (b); erythrocyte morphology of mice blood after incubating the blood with a final concentration of 5 mg/mL PHEMA-g-(PLA-DPPE) copolymers for 3 hours (c), erythrocyte morphology of mice blood after incubating the blood with a final concentration of 15 mg/mL PHEMA-g-(PLA-DPPE) copolymer for 3 hours.

**Abbreviations:** PHEMA, poly (2-hydroxyethyl methacrylate); PLA, poly (lactide)-I; DPPE, 2-dipalmitoyl-sn-glycero-3-phosphoethanolamine.

limited due to its poor solubility. Further, the solubilizing agent Cremophor EL may cause severe anaphylactic hypersensitivity reactions, hyperlipidemia, abnormal lipoprotein patterns, aggregation of erythrocytes, and peripheral neuropathy in patients.<sup>43</sup> Accordingly, biocompatible polymeric paclitaxel-loaded nanoparticles without Cremophor EL have been developed to overcome these obstacles. Biocompatible and biodegradable polymers are particularly attractive for application in drug delivery systems. Once introduced into

the human body, they do not require removal or additional manipulation. The results of the cytotoxicity assay demonstrate that the patterns of cell viability in the presence of paclitaxel-loaded nanoparticles and the free drug were similar. This suggests that paclitaxel entrapped in nanoparticles was as potent as free paclitaxel in the tested tumor cell line. Further, the polymeric nanoparticles used in our study had superior biocompatibility and may be a favorable alternative to the formulation approach involving Cremophor EL, thus

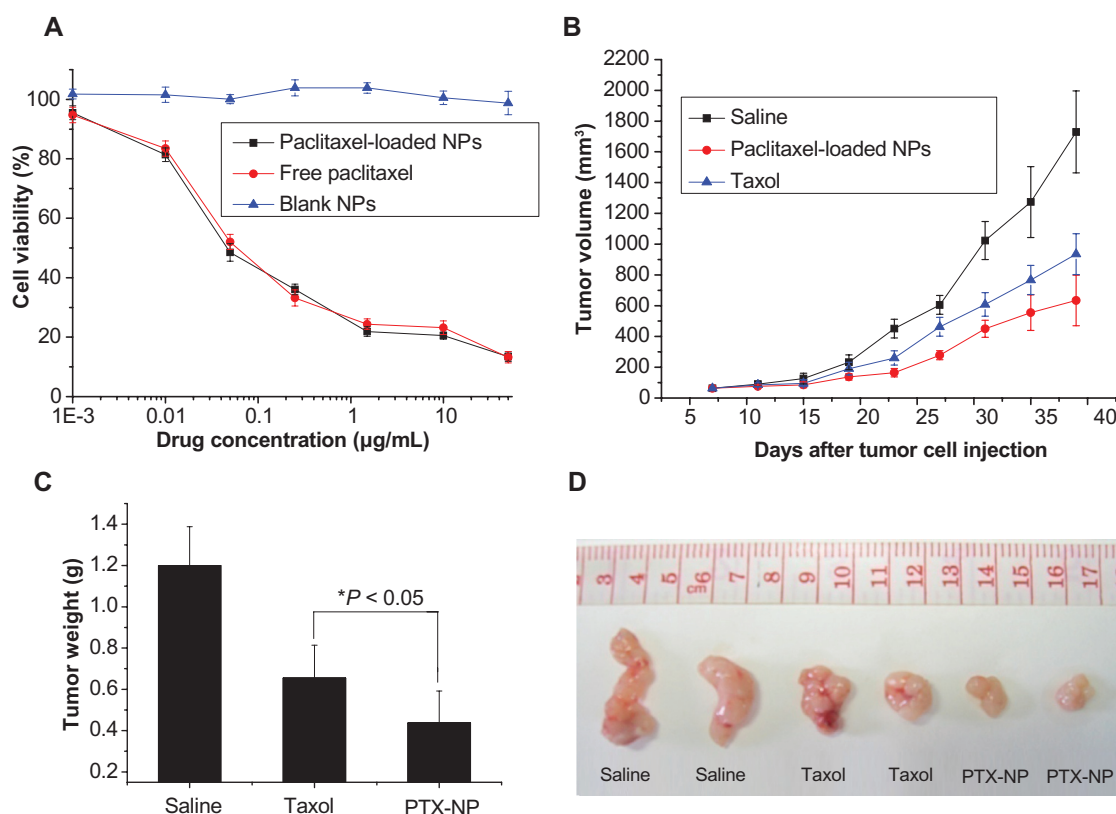


**Figure 5** (A) Inhibition of cancer cell proliferation by free paclitaxel and paclitaxel-loaded PHEMA-PLA-DPPE nanoparticles. Inhibition of MCF-7 cell proliferation by free paclitaxel, paclitaxel-loaded nanoparticles, or empty nanoparticles after 48 hours of incubation at 37°C. The concentration of empty nanoparticles used was equal to the concentration of paclitaxel-loaded nanoparticles. Tumor volume (B) and tumor weight (C) of MCF-7 tumor-bearing female nude mice treated with saline, paclitaxel, or paclitaxel-loaded PHEMA-g-(PLA-DPPE) nanoparticles. Data are presented as the mean  $\pm$  standard deviation ( $n = 4$ ). (D) Representative images of excised tumors from mice treated with saline, free paclitaxel, or paclitaxel-loaded PHEMA-g-(PLA-DPPE) nanoparticles.

**Abbreviations:** PHEMA, poly (2-hydroxyethyl methacrylate); PLA, poly (lactide)-I; DPPE, 2-dipalmitoyl-sn-glycero-3-phosphoethanolamine.

allowing for reduction of toxicity. In chemotherapy, maintenance of drug levels in the body is usually achieved by repeated administrations. Despite the effectiveness of these treatments, dose peaks at administration times are unavoidably alternated with subtherapeutic drug levels. Therefore, the impossibility of controlling the drug level over a long period of time constitutes an important drawback. We have compared free paclitaxel and paclitaxel-loaded PHEMA-g-(PLA-DPPE) nanoparticles in MCF-7 cells and found them to have comparable cytotoxic efficacy. Therefore, in our experiment, the nanoparticles exert their effects by changing the pharmacokinetics of paclitaxel at the animal level rather than by changing drug efficacy at the cellular level. In the case of solid tumors with compromised and leaky vasculature, localized drug delivery can be achieved largely as a function of particle size, and is referred to as “passive targeting”. The PHEMA-g-(PLA-DPPE) nanoparticles used in our experiment had a particle size of about 200 nm. It has been reported that nanoparticles with a size around 200 nm would readily accumulate and be retained in the tumor interstitium because of the

enhanced permeability and retention effect, which is further facilitated by the lack of a draining lymphatic system in tumor tissues.<sup>44–46</sup> The circulation half-life of drug in the blood can be improved by coating it with a neutral or anionic shell.<sup>47</sup> In this case, we speculate that the hydrophilic polymer PHEMA shields charges and hydrophobic residues, reducing protein opsonization in vivo and thereby helps the nanoparticle to escape the reticuloendothelial system. This allows for prolonged circulation of paclitaxel and an extended drug effect. After entering the circulation, passive targeting of drugs to tumor tissue is achieved by the negatively charged PHEMA-g-(PLA-DPPE) nanoparticles (zeta potential  $-23.4$  mV). Previous reports have confirmed that PEG-PE polymers could form stable micelles in aqueous media and had longevity in the systemic circulation.<sup>29</sup> From the results of our animal experiments, paclitaxel-loaded PHEMA-g-(PLA-DPPE) nanoparticles had a good inhibitory effect on tumor tissue, which we speculate may be due to the long circulation time and biocompatibility of the DPPE segment. According to the enhanced permeation and retention concept,



biocompatible macromolecules accumulate at much higher concentrations in tumor tissues than in normal tissues or organs, and at even higher levels than in plasma. The mechanism by which pH-responsive polymeric paclitaxel-loaded PHEMA-g-(PLA-DPPE) nanoparticles outperform the free drug may be due to controlled drug release, achieved by slowing drug leakage during circulation in the blood. Blood has a pH of 7.4, and accumulates and releases the drug after reaching tumor areas which have a more acidic pH. A slower release rate at pH 7.4 than at pH 5 gives the drug maximum protection during its circulation in the blood and other body fluids, and thereby maintains an effective therapeutic concentration for a longer period of time and increases overall accumulation of the drug in the tumor tissue.

## Conclusion

In the current study, we developed a novel amphiphilic PHEMA-g-(PLA-DPPE)-based nanocarrier for delivery of the hydrophobic drug, paclitaxel. The paclitaxel-loaded copolymer nanoparticles fabricated using the emulsion-solvent evaporation method were shown to have the following properties: bioapplication and bioabsorbability of PHEMA derivatives; markedly improved solubility of paclitaxel and without use of Cremophor EL; high loading capacity; and a controlled drug release profile. Paclitaxel-loaded polymeric nanoparticles were as cytotoxic to MCF-7 cells as free paclitaxel, while no cytotoxicity was observed to the polymers themselves. In mice, paclitaxel-loaded nanoparticles showed enhanced antitumor efficacy compared with free paclitaxel. Based on these results, it is expected that this PHEMA-g-(PLA-DPPE)-based drug packaging nanocarrier technology would provide a new strategy for delivery of hydrophobic antitumor therapeutics.

## Acknowledgments

This work was financially supported by the National Key Basic Research Program of China (MOST 973 project 2009CB930200) and the program of National Natural Science Foundation of China (30970784, 81171455). The authors are grateful for the support of the Chinese Academy of Sciences Hundred Talents Program and the Chinese Academy of Sciences Knowledge Innovation Program.

## Disclosure

The authors report no conflicts of interest in this work.

## References

1. Brannon-Peppas L, Blanchette JO. Nanoparticle and targeted systems for cancer therapy. *Adv Drug Deliv Rev*. 2004;56(11):1649–1659.
2. Torchilin VP. Lipid-core micelles for targeted drug delivery. *Curr Drug Deliv*. 2005;2(4):319–327.
3. Torchilin VP. Structure and design of polymeric surfactant-based drug delivery systems. *J Control Release*. 2001;73(2–3):137–172.
4. Arica MY, Bayramoglu G, Arica B, et al. Novel hydrogel membrane based on copoly(hydroxyethyl methacrylate/p-vinylbenzyl-poly(ethylene oxide)) for biomedical applications: properties and drug release characteristics. *Macromol Biosci*. 2005;5(10):983–992.
5. Flynn L, Dalton PD, Shoichet MS. Fiber templating of poly(2-hydroxyethyl methacrylate) for neural tissue engineering. *Biomaterials*. 2003;24(23):4265–4272.
6. Khutoryanskaya OV, Mayeva ZA, Mun GA, et al. Designing temperature-responsive biocompatible copolymers and hydrogels based on 2-hydroxyethyl(meth)acrylates. *Biomacromolecules*. 2008;9(12):3353–3361.
7. Prasitsilp M, Siriwittayakorn T, Molloy R, et al. Cytotoxicity study of homopolymers and copolymers of 2-hydroxyethyl methacrylate and some alkyl acrylates for potential use as temporary skin substitutes. *J Mater Sci Mater Med*. 2003;14(7):595–600.
8. Studenovska H, Slouf M, Rypacek F. Poly(HEMA) hydrogels with controlled pore architecture for tissue regeneration applications. *J Mater Sci Mater Med*. 2008;19(2):615–621.
9. Vert M, Li SM, Spenlehauer G, et al. Bioresorbability and biocompatibility of aliphatic polyesters. *J Mater Sci Mater Med*. 1992;3(6):432–446.
10. Wu DX, Zhao CZ, Tian J, et al. Synthesis of PLLA-PEOMA comb-block-comb type molecular brushes based on AGET ATRP and ring-opening polymerization. *Polym Int*. 2009;58(11):1335–1340.
11. Zhao CZ, Wu DX, Huang N, et al. Crystallization and thermal properties of PLLA comb polymer. *J Polym Sci B Polym Phys*. 2008;46(6):589–598.
12. Cretu A, Kipping M, Adler HJ, et al. Synthesis and characterization of hydrogels containing biodegradable polymers. *Polym Int*. 2008;57(7):905–911.
13. Shinoda H, Matyjaszewski K. Structural control of poly(methyl methacrylate)-g-poly(lactic acid) graft copolymers by atom transfer radical polymerization (ATRP). *Macromolecules*. 2001;34(18):6243–6248.
14. Wolf FF, Friedemann N, Frey H. Poly(lactide)-block-Poly(HEMA) block copolymers: an orthogonal one-pot combination of ROP and ATRP, using a bifunctional initiator. *Macromolecules*. 2009;42(15):5622–5628.
15. Clement B, Trimaille T, Alluin O, et al. Convenient access to biocompatible block copolymers from SG1-based aliphatic polyester macro-alkoxyamines. *Biomacromolecules*. 2009;10(6):1436–1445.
16. Cretu A, Gattin R, Brachais L, et al. Synthesis and degradation of poly(2-hydroxyethyl methacrylate)-graft-poly(epsilon-caprolactone) copolymers. *Polym Degrad Stab*. 2004;83(3):399–404.
17. Wu X, Griffin P, Price GJ, et al. Preparation and in vitro evaluation of topical formulations based on polystyrene-poly-2-hydroxyl methacrylate nanoparticles. *Mol Pharm*. 2009;6(5):1449–1456.
18. Schappacher M, Fur N, Guillaume SM. Poly(methyl methacrylate)-poly(caprolactone) AB and ABA block copolymers by combined ring-opening polymerization and atom transfer radical polymerization. *Macromolecules*. 2007;40(25):8887–8896.
19. Zhang Q, Remsen EE, Wooley KL. Shell cross-linked nanoparticles containing hydrolytically degradable, crystalline core domains. *J Am Chem Soc*. 2000;122(15):3642–3651.
20. Pifftis D, Pitsikalis M, Hadjichristidis N. Miktoarm star copolymers of poly(epsilon-caprolactone) from a novel heterofunctional initiator. *J Polym Sci A Polym Chem*. 2007;45(22):5164–5181.
21. Beers KL, Gaynor SG, Matyjaszewski K, et al. The synthesis of densely grafted copolymers by atom transfer radical polymerization. *Macromolecules*. 1998;31(26):9413–9415.
22. Danhier F, Vroman B, Lecourtier N, et al. Targeting of tumor endothelium by RGD-grafted PLGA-nanoparticles loaded with paclitaxel. *J Control Release*. 2009;140(2):166–173.
23. Wang Y, Ng YW, Chen Y, et al. Formulation of superparamagnetic iron oxides by nanoparticles of biodegradable polymers for magnetic resonance imaging. *Adv Funct Mater*. 2008;18(2):308–318.



24. Baras B, Benoit MA, Gillard J. Parameters influencing the antigen release from spray-dried poly(DL-lactide) microparticles. *Int J Pharm*. 2000;200(1):133–145.
25. Perez C, Sanchez A, Putnam D, et al. Poly(lactic acid)-poly(ethylene glycol) nanoparticles as new carriers for the delivery of plasmid DNA. *J Control Release*. 2001;75(1–2):211–224.
26. Suh H, Hwang YS, Lee JE, et al. Behavior of osteoblasts on a type I atelocollagen grafted ozone oxidized poly L-lactic acid membrane. *Biomaterials*. 2001;22(3):219–230.
27. Lukyanov AN, Elbayoumi TA, Chakilam AR, et al. Tumor-targeted liposomes: doxorubicin-loaded long-circulating liposomes modified with anti-cancer antibody. *J Control Release*. 2004;100(1):135–144.
28. Maeda N, Takeuchi Y, Takada M, et al. Anti-neovascular therapy by use of tumor neovasculture-targeted long-circulating liposome. *J Control Release*. 2004;100(1):41–52.
29. Tang N, Du G, Wang N, et al. Improving penetration in tumors with nanoassemblies of phospholipids and doxorubicin. *J Natl Cancer Inst*. 2007;99(13):1004–1015.
30. Amado E, Kerth A, Blume A, et al. Infrared reflection absorption spectroscopy coupled with Brewster angle microscopy for studying interactions of amphiphilic triblock copolymers with phospholipid monolayers. *Langmuir*. 2008;24(18):10041–10053.
31. Weiss RB, Donehower RC, Wiernik PH, et al. Hypersensitivity reactions from Taxol. *J Clin Oncol*. 1990;8(7):1263–1268.
32. Danhier F, Lecouturier N, Vroman B, et al. Paclitaxel-loaded PEGylated PLGA-based nanoparticles: in vitro and in vivo evaluation. *J Control Release*. 2009;133(1):11–17.
33. Wu Y, Zheng YL, Yang WL, et al. Synthesis and characterization of a novel amphiphilic chitosan-poly(lactide) graft copolymer. *Carbohydr Polym*. 2005;59(2):165–171.
34. Wang Z, Chui WK, Ho PC. Design of a multifunctional PLGA nanoparticulate drug delivery system: evaluation of its physicochemical properties and anticancer activity to malignant cancer cells. *Pharm Res*. 2009;26(5):1162–1171.
35. Gref R, Quellec P, Sanchez A, et al. Development and characterization of CyA-loaded poly(lactic acid)poly(ethylene glycol)PEG micro- and nanoparticles. Comparison with conventional PLA particulate carriers. *Eur J Pharm Biopharm*. 2001;51(2):111–118.
36. Lebouc F, Dez I, Madec PJ. NMR study of the phosphonomethylation reaction on chitosan. *Polymer*. 2005;46(2):319–325.
37. Sabesan S, Neira S. Synthesis of glycosyl phosphates and azides. *Carbohydr Res*. 1992;223:169–185.
38. Connor J, Yatvin MB, Huang L. pH-sensitive liposomes: acid-induced liposome fusion. *Proc Natl Acad Sci U S A*. 1984;81(6):1715–1718.
39. Gerasimov OV, Boomer JA, Qualls MM, et al. Cytosolic drug delivery using pH- and light-sensitive liposomes. *Adv Drug Deliv Rev*. 1999;38(3):317–338.
40. Mainardes RM, Evangelista RC. PLGA nanoparticles containing praziquantel: effect of formulation variables on size distribution. *Int J Pharm*. 2005;290(1–2):137–144.
41. Duncan R. Polymer conjugates as anticancer nanomedicines. *Nat Rev Cancer*. 2006;6(9):688–701.
42. Bae Y, Fukushima S, Harada A, et al. Design of environment-sensitive supramolecular assemblies for intracellular drug delivery: polymeric micelles that are responsive to intracellular pH change. *Angew Chem Int Ed Engl*. 2003;42(38):4640–4643.
43. Gelderblom H, Verweij J, Nooter K, et al. Cremophor EL: the drawbacks and advantages of vehicle selection for drug formulation. *Eur J Cancer*. 2001;37(13):1590–1598.
44. Maeda H, Seymour LW, Miyamoto Y. Conjugates of anticancer agents and polymers: advantages of macromolecular therapeutics in vivo. *Bioconj Chem*. 1992;3(5):351–362.
45. Maeda H, Wu J, Sawa T, et al. Tumor vascular permeability and the EPR effect in macromolecular therapeutics: a review. *J Control Release*. 2000;65(1–2):271–284.
46. Maruyama K. Intracellular targeting delivery of liposomal drugs to solid tumors based on EPR effects. *Adv Drug Deliv Rev*. 2011;63(3):161–169.
47. Shutao G, Leaf H. Nanoparticles escaping RES and endosome: challenges for siRNA delivery for cancer therapy. *J Nanomater*. 2011; 2011.

## Supplementary details on copolymer synthesis and characterization

Supplementary Figure S1A–C show the  $^{13}\text{C}$  NMR spectra for PHEMA, PHEMA-PLA, and PHEMA-g-(PLA-DPPE) copolymer, respectively. Compared with PHEMA (Supplementary Figure S1A), the  $^{13}\text{C}$  NMR spectra of the PHEMA-PLA copolymer (Supplementary Figure S1B) show that the signals at about 160–175 ppm were attributed to the

C=O group carbon peak of PLA. The signals at approximately 64 and 69 ppm were assigned to the  $-\text{CH}$  group carbon peak of the PLA moiety located at the terminal groups and repeat units in the chain. The signals at approximately 15 and 20 ppm were attributed to the  $-\text{CH}_3$  group carbon peak of the PLA moiety located at repeat units and the terminal groups. Compared with PHEMA-PLA (Supplementary Figure S1B), PHEMA-g-(PLA-DPPE) (Supplementary Figure S1C) showed a peak at about 9.0 ppm. This was attributed to

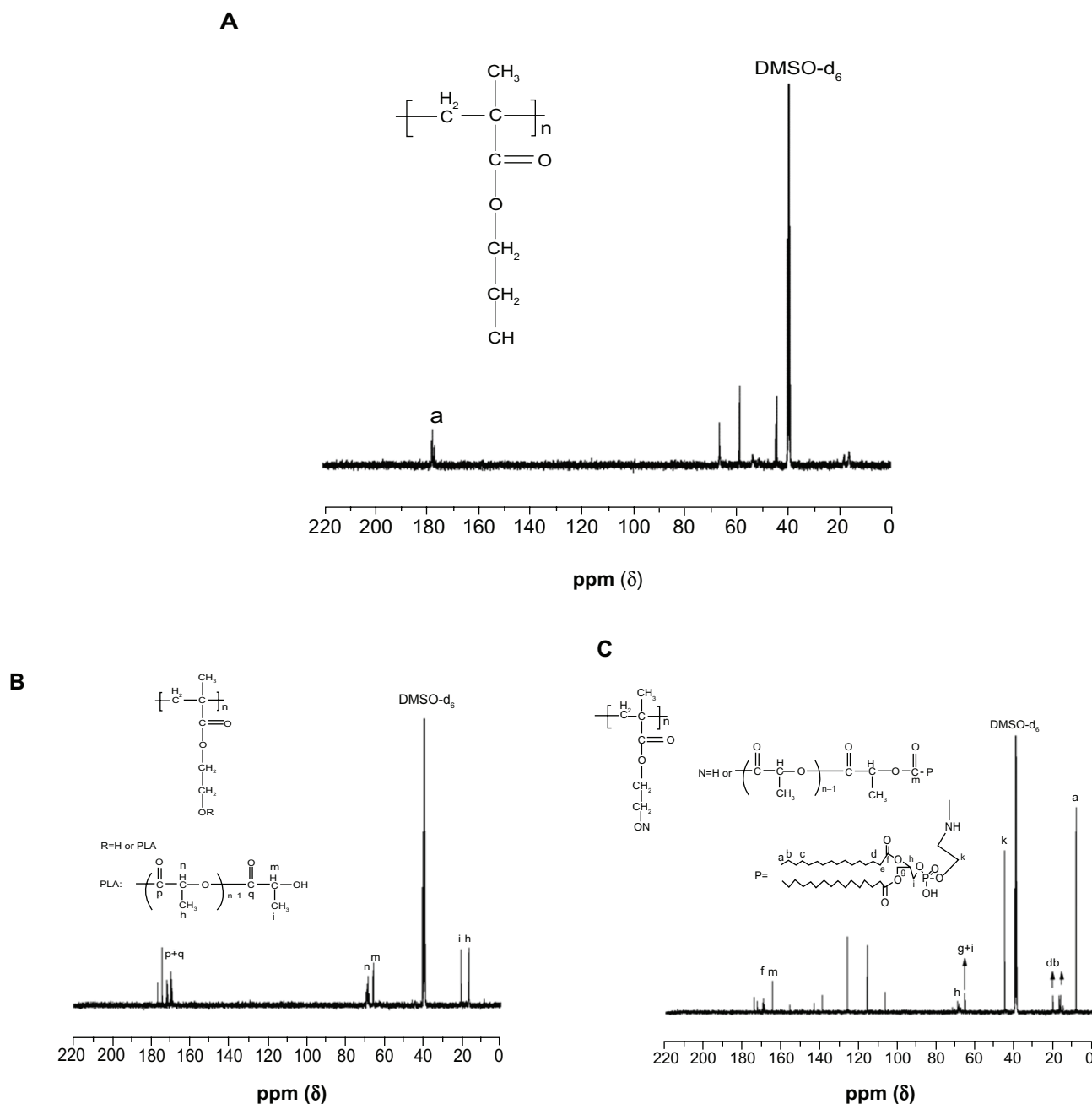


**Figure S1**  $^{13}\text{C}$  NMR spectra of PHEMA (A), PHEMA-PLA (B), and PHEMA-g-(PLA-DPPE) copolymers (C).

**Abbreviations:** PHEMA, poly (2-hydroxyethyl methacrylate); PLA, poly (lactide)-I; DPPE, 2-dipalmitoyl-sn-glycero-3-phosphoethanolamine.

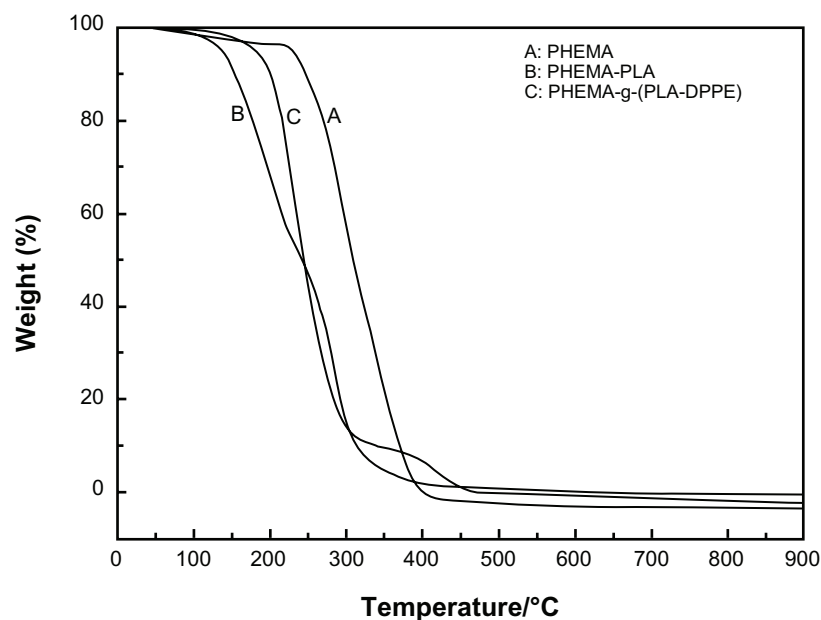


**Figure S2** Thermogravimetric analysis profiles of (A) PHEMA, (B) PHEMA-PLA, and (C) PHEMA-g-(PLA-DPPE) copolymers.  
**Abbreviations:** PHEMA, poly (2-hydroxyethyl methacrylate); PLA, poly (lactide)-I; DPPE, 2-dipalmitoyl-sn-glycero-3-phosphoethanolamine.

the  $-\text{CH}_3$  group carbon peak of the DPPE moiety located at the terminal groups. The signals at about 15–20 ppm were assigned to the  $-\text{CH}_2$  group carbon peak of the DPPE moiety. The signals at about 170 ppm were assigned to the  $\text{C}=\text{O}$  group carbon peak of PHEMA-g-(PLA-DPPE). All other absorption peaks were attributed to the carbon peaks of the DPPE moiety.

The thermal properties of polymers were examined by thermogravimetric analysis. Figure S2 shows the thermogravimetric analysis for PHEMA, PHEMA-PLA, and PHEMA-g-(PLA-DPPE) copolymers, respectively. As shown in Figure S2, the PHEMA-PLA and the PHEMA-g-(PLA-DPPE)

copolymers had a lower thermal degradation temperature than the original PHEMA. Rapid weight loss appeared in the thermogravimetric analysis curves for copolymers in the thermal degradation range above 150°C, and lower than PHEMA at 250°C. We can conclude that the introduction of PLA and DPPE into the copolymer led to a decrease in the thermal stability of the original PHEMA.

## Abbreviations

PHEMA, poly (2-hydroxyethyl methacrylate; NMR, nuclear magnetic resonance; PLA, poly (lactide)-1; DPPE, 2-dipalmitoyl-sn-glycero-3-phosphoethanolamine.

## International Journal of Nanomedicine

### Publish your work in this journal

The International Journal of Nanomedicine is an international, peer-reviewed journal focusing on the application of nanotechnology in diagnostics, therapeutics, and drug delivery systems throughout the biomedical field. This journal is indexed on PubMed Central, MedLine, CAS, SciSearch®, Current Contents®/Clinical Medicine, Journal

Submit your manuscript here: <http://www.dovepress.com/international-journal-of-nanomedicine-journal>

Citation Reports/Science Edition, EMBase, Scopus and the Elsevier Bibliographic databases. The manuscript management system is completely online and includes a very quick and fair peer-review system, which is all easy to use. Visit <http://www.dovepress.com/testimonials.php> to read real quotes from published authors.

## Dovepress